Distinguishing Tunneling Pathways for Two Chiral Conformer Pairs of 1,3-Propanediol from the Microwave Spectrum

D. F. Plusquellic,*,† F. J. Lovas,†,‡ Brooks H. Pate,‡ Justin L. Neill,‡ Matthew T. Muckle,‡ and Anthony J. Remijan‡,§

Optical Technology Division, National Institute of Standards and Technology, Gaithersburg, Maryland 20899-8441, USA, Center for Chemistry of the Universe, Department of Chemistry, Univeristy of Virginia, McCormack Rd, P.O. Box 400319, Charlottesville, Virginia 22904-4319, National Radio Astronomy Observatory, 520 Edgemont Rd., Charlottesville, Virginia 22903-2475

Received: August 5, 2009; Revised Manuscript Received: September 24, 2009

Downloaded by BOULDER LABORATORIES LBRY on September 3, 2015 | http://pubs.acs.org
Publication Date (Web): October 13, 2009 | doi: 10.1021/jp907564y

The microwave spectrum of the sugar alcohol 1,3-propanediol ($CH_2OHCH_2CH_2OH$) has been measured over the frequency range 6.7 to 25.4 GHz using both cavity and broadband microwave spectrometers. The tunneling splittings from two structurally chiral conformer (enantiomeric) pairs of 1,3-propanediol have been fully resolved and assigned. The tunneling frequency of the lowest-energy inverting pair is 5.4210(28) MHz and found to increase by more than 7-fold to 39.2265(24) MHz for the higher-energy form. From the observed selection rules, three possible inversion pathways along the two OH concerted torsional modes have been identified and theoretically investigated. Quantum chemical calculations (MP2/aug-cc-pVTZ level) have been performed on the eight lowest-energy forms and three transition-state structures. Two of these pathways cross through C_S transition states associated with each of the enantiomeric pairs and a third common pathway of lowest energy has a transition state of C_1 symmetry. For only the C_1 pathway is good agreement found between predictions from a 1D WKB analysis and the observed tunneling frequencies and 7-fold ratio. The conformer interconversion barrier is calculated to be about 3-fold smaller than that for the inversion suggesting the wave functions of the four inversion levels are partially delocalized over the four surface minima. Accurate dipole moment components have also been obtained from Stark effect measurements for the lowest-energy form.

1. Introduction

The simplest sugar, glycolaldehyde (CH_2OHCHO),[1] and its diol derivative, ethylene glycol (CH_2OHCH_2OH),[2] have been detected toward the interstellar molecular cloud, Sgr B2 (N-LMH). The identification of sugar alcohols and sugar acids in the Murchinson and Murray meteorites[3] has increased the interest in investigating interstellar sugars and their derivatives. 1,3-Propanediol is one of two forms of propanediol, the other being 1,2-propanediol, and is related to ethylene glycol by the insertion of a methylene group between the carbon atoms. The propanediols are important industrial chemicals that serve as alternate antifreezes to ethylene glycol. They are also used in composites, adhesives, paints, and laminates.

In our recent FTMW study of 1,2-propanediol,[4] seven different conformations were observed in the jet-cooled spectrum. These seven forms divided into four pairs where members of the pair differed by the simple ≈115° rotation of the hydrogen bond accepting (or free) OH group (the eighth highest energy form was not detected). The final conformer temperatures relative to the source temperature were derived from the ab initio energies and the relative overall intensities and suggested facile interconversion cooling routes by free OH rotation to the lower-energy member of the pair. Within this collisional cooling model, the degree of relaxation appeared to depend on the magnitude of the interconversion barrier where higher barriers led to less effective cooling of the conformer population.

The symmetric isomer of interest here, 1,3-propanediol, also exists in several possible low-energy forms. The microwave spectrum of one conformer (at lowest energy) was previously investigated in the frequency range from 60 to 78 GHz using a free-jet microwave absorption spectrometer.[5] We have augmented the data on this conformer by a new series of measurements in the 6.5 to 25.5 GHz frequency range using the NIST cavity FTMW spectrometer. Furthermore, the high sensitivity of chirped-pulse FTMW measurements performed at the University of Virginia have revealed the presence of a second conformer. The spectra of both conformers display tunnelling splitting that result from interconversion between structurally chiral forms. Independent of the collisional cooling dynamics, these splittings are shown to provide information about the interconversion pathways when coupled with predictions from a simple WKB model and high-level ab initio calculations[6] (MP2[7]/aug-cc-pVTZ[8]) performed on the lowest-energy theoretical conformers first reported by Vázquez et al.[9] at the 4−21G level. Such models of facile OH interconversion may have wider reaching consequences in the understanding of the physical and thermal transport properties of other sugar-alcohols and polysaccharides.[10]

2. Experimental Details

The initial measurements were carried out using a Fabry−Perot cavity, pulsed-nozzle Fourier-transform microwave spectrometer of the Balle-Flygare type[11] designed by Lovas and Suenram.[12,13]

* To whom correspondence should be addressed. E-mail: David.Plusquellic@nist.gov.
† National Institute of Standards and Technology.
‡ Univeristy of Virginia.
§ National Radio Astronomy Observatory.

10.1021/jp907564y CCC: $40.75 © 2009 American Chemical Society
Published on Web 10/13/2009

Downloaded by BOULDER LABORATORIES LBRY on September 3, 2015 | http://pubs.acs.org
Publication Date (Web): October 13, 2009 | doi: 10.1021/jp907564y

This design employs a coaxial-oriented nozzle[14] and PC-based system for timing, mirror movement, nozzle control, synthesizer tuning, and signal processing and uses the *FTMW++* software system designed by Grabow.[15] 1,3-propanediol is a colorless liquid and has a low vapor pressure at room temperature. Therefore, to obtain a sufficient signal, the sample was heated up to 90 °C in a nozzle equipped with a reservoir. The jet-cooled expansion was produced by mixing the vapor with 20% helium and 80% neon carrier gas (by volume) at a total pressure of 100 kPa (1 atm) and then injecting it into the cavity through a 1 mm nozzle orifice along the axis of the Fabry−Perot cavity and parallel to the microwave field. Molecular transitions, observed as Doppler doublets, had line widths of 5 kHz, and the frequency measurement uncertainties were estimated to be 2 kHz for the cavity FTMW.

The chirped-pulse FTMW spectrometer at the University of Virginia was used to provide a deep integration survey scan from 6.5 to 18 GHz. This spectrometer was recently described by Brown et al.[16] In the present experiments, the B configuration of the spectrometer described in ref 16 was employed with an additional upgrade of the arbitrary waveform generator (AWG) to a 24 Gs/s sample rate (Tektronix AWG7122B).[17] The chirped microwave excitation pulse was created by mixing a linear sweep pulse generated by the AWG with a 18.95 GHz phase-locked dielectric resonator oscillator (PDRO). The AWG pulse sweeps the frequency range of 12 GHz to 500 MHz with a duration of 1 μs creating a microwave pulse that covers the 6.95 to 18.45 GHz frequency range following frequency up-conversion with the PDRO.

Two strategies to reduce sample consumption described in ref 16 were implemented. Sample introduction into the vacuum chamber used two pulsed valve sources operated with 700 μs pulse duration. The nozzles inject the sample perpendicular to the axis of microwave propagation. For each sample injection cycle, 10 separate broadband rotational spectra were acquired. The individual broadband chirped pulses were separated by 25 μs. The rotational free induction decay was acquired for 20 μs following each 1 μs excitation pulse. The repetition rate for the sample injection was 0.6 Hz and is limited by the data-processing rate of the digital oscilloscope. A total of 424 000 rotational spectra of 1,3-propanediol were acquired in 42 400 injection cycles with a total measurement duration of approximately 21 h. The sample conditions for the broadband FTMW measurements were the same as those for the cavity FTMW measurements described above but a repetition rate of 4 Hz was used and a single spectrum was acquired for each sample injection.

3. Ab Initio Calculations

Vázquez et al.[9] reported optimized geometries for 25 conformers of 1,3-propanediol from ab initio calculations at the 4-21G level. We use the conformer labeling scheme employed there as well as their atom numbering for easier comparisons. This labeling scheme provides a four character label, xXXx, where X (capital for the OCCC and CCCO dihedral angles and lower case for the hydroxyl hydrogens or HOCC angles) can be G, or G', depending on the gauche position of the atom considered with respect to a reference bond. G and G' indicate an anticlockwise or a clockwise rotation from the cis (syn) position of O2−C3−C4-C5 and C3−C4−C5−O6 dihedral angles for the X values and similarly for the HOCC dihedral angles represented by x whose values may be g, g', t, or t'. The first x represents the position of the hydroxyl hydrogen H1 with respect to C4, the second x the position of H7 with respect to C4.

We have re-examined the eight lowest-energy forms whose calculated energies were below 7.6 kJ/mol (560 cm^{-1}). Geometry optimizations were performed at the MP2[7]/aug-cc-pVTZ[8] level on the eight lowest-energy conformers of 1,3-propanediol using the *Gaussian 03 Quantum Chemistry Package*.[6,17] All eight of the fully optimized geometric isomers are shown in Figure 1. All geometries were verified as true minima in subsequent calculations of the analytical second derivatives. In Table 1, the relative energies of the eight conformers with and without zero-point-energy (ZPE) corrections are summarized. The most noteworthy change from the previous results is the substantial reduction in the relative energy of conformer V (especially with consideration of the zero-point energy correction) moving it to third place in the energy order. Also reported in Table 1 are the predicted rotational constants and dipole moment components that were used to aid the identification of the experimentally observed forms. The structural parameters are given in Tables S1−S4 of the Supporting Information according to the labeling given in Figure 1.

4. Results and Analysis

Initial spectral predictions were made based on the rotational constants reported in a study by Caminati et al.[5] A comparison with the observed spectrum permitted the immediate assignment of this conformer over the frequency range of 6.7 to 25.4 GHz. To fit all of the observed transitions, however, a model to account for tunneling on a symmetric double minimum surface was necessary where the lowest two inversion levels, 0^+ and 0^-, were split by 5.4 MHz In this case, all *b*- and *c*-type transitions were assigned as pure rotational transitions within each inversion level ($0^+ \rightarrow 0^+$, $0^- \rightarrow 0^-$) and *a*-type lines were assigned to transitions that crossed between the inversion states ($0^+ \rightarrow 0^-$, $0^- \rightarrow 0^+$). The complete data set that included 74 new rotational and inversion-level assignments (not counting degenerate ones twice) were fitted together with the data from Caminati et al.[5] using Pickett's *SPFIT* program.[18] The weighted standard deviation of the fit was 0.97. The best-fit inversion-level splitting and rotational constants of the two tunneling states are given in Table 2. Whereas the constants *A* and *B* and distortion parameters for the two levels are the same within the uncertainties, *C* for the 0^- level is slightly smaller (and corresponding moment of inertial slightly larger) than that of the 0^+ level as might be expected from the nodal character of these two wave functions. The calculated constants for conformer I in Table 2 are in good agreement with the observed values. A summary of all transitions measured here and by Caminati et al.[5] are given in Table S5 of the Supporting Information.

Whereas conformer I was easily detected in this spectrum using the cavity FTMW instrument with a 20 beam-pulse average, the signal-to-noise was insufficient to detect transitions of conformer II. Here, a deep integration capacity of the broadband spectrometer was needed to obtain sufficient detection sensitivity. The same selection rules used to assign conformer I were applied to this spectrum. However, in this case, the *a*-type transitions were split by 78.5 MHz, which is more than seven times larger than that observed for conformer I. Using predictions from this initial assignment, additional averaging was performed on transitions using the cavity FTMW instrument from 13 to 21.6 GHz. At the resolution of these latter measurements and because of the much larger inversion-level splitting, some of the *b*- and *c*-type pure rotational transitions

Downloaded by BOULDER LABORATORIES LBRY on September 3, 2015 | http://pubs.acs.org
Publication Date (Web): October 13, 2009 | doi: 10.1021/jp907564y

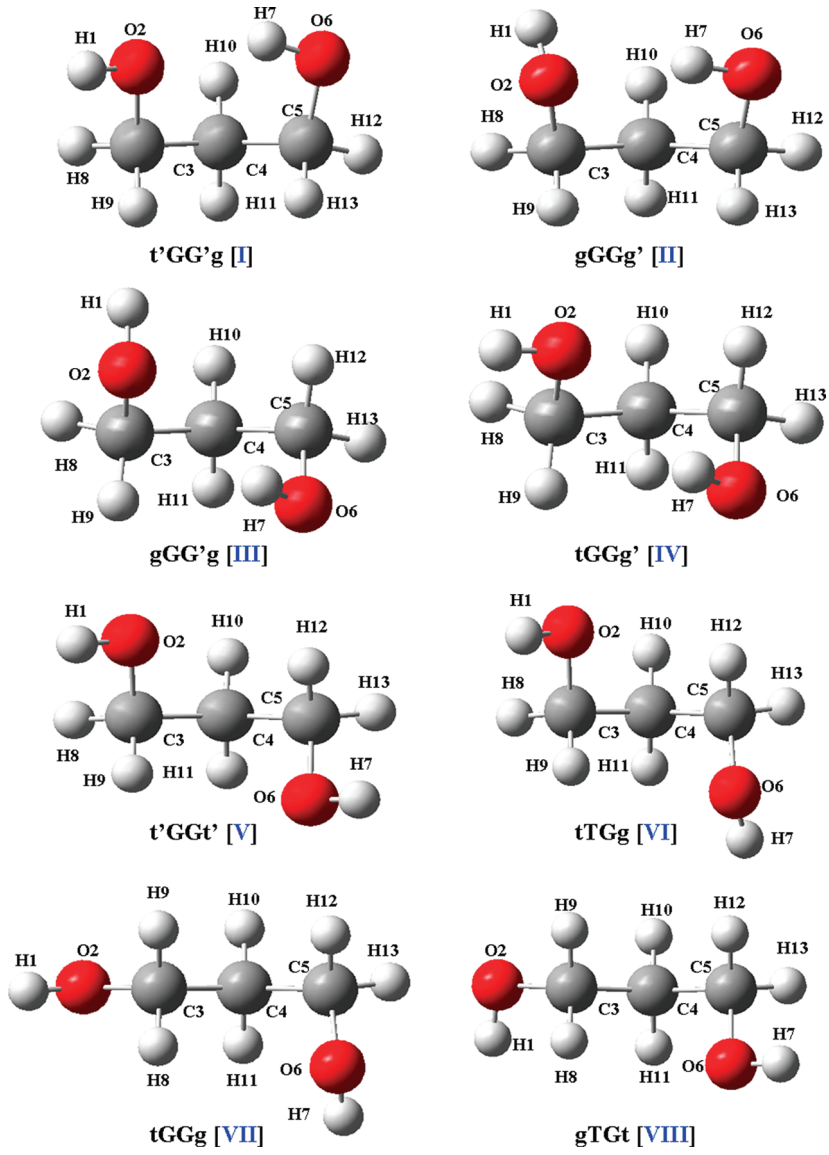

Figure 1. Conformers I through VIII of 1,3-propanediol given in order of their relative zero-point corrected energies determined from ab initio MP2/aug-cc-pVTZ calculations. Atom labels correlate with structural parameters given in Tables S1−S4 of the Supporting Information.

TABLE 1: Theoretical Rotational Constants, Dipole Moments[a], and Energies for the 1,3-Propanediol Conformers at the MP2/aug-cc-pVTZ Level of Theory

#	label	*A*/MHz	*B*/MHz	*C*/MHz	μ_a/D	μ_b/D	μ_c/D	ΔE/cm^{-1}	ΔE^b/cm^{-1}	ΔE^b/kJmol^{-1}
I	t'GG'g	7712.7	3964.7	2894.3	3.01	1.62	1.16	0	0	0.0
II	gGG'g	7581.4	3960.2	2888.1	1.80	2.13	−0.65	82	107	1.28
III	gGGg'	7781.4	3594.6	3037.8	−1.55	1.71	1.19	442	423	5.06
IV	tGGg'	7808.7	3654.3	3078.1	−2.35	0.40	−0.28	561	516	6.17
V	t'GGt'	9055.4	3045.7	2867.1	0.0	−0.40	0.0	429	287	3.43
VI	t'GGg	9172.4	2976.8	2811.9	0.18	1.36	1.35	625	480	5.74
VII	tT'Gg	13243.9	2417.8	2235.9	−0.06	0.04	−0.06	808	643	7.69
VIII	gTGt'	13268.6	2429.8	2245.2	2.26	0.62	−0.08	827	661	7.90

[a] Zero-point-energy (ZPE) corrections included. Conversion factor 1 kJmol^{-1} = 83.594 cm^{-1}. [b] For SI units, 1D (Debye) = 3.336 × 10^{-30} Cm.

were slightly split. The final fit from *SPFIT*[18] included a total of 69 transitions and gave an rms deviation of 4.3 kHz. The fitted parameters are given in Table 3. In this case, only one set of centrifugal distortion parameters were determined for both inversion levels. All of assigned transitions of conformer II are given in Table S6 of the Supporting Information.

The high quality of the data from the broadband scan made possible the assignment of spectra from the individual ^{13}C isotopologues of conformer I. Because atoms C_3 and C_5 are not symmetrically equivalent, the ^{13}C substitution effectively quenches the tunneling and the two isotopologues give rise to uncoupled asymmetric top spectra. However, tunneling splittings are again expected and observed for the central $^{13}C_4$ substitution. The fitted parameters for the $^{13}C_3$ and the $^{13}C_5$ species are listed in Table 4. For comparison, the calculated rotational constants were derived from the ab initio structure of conformer I with the appropriate ^{13}C mass used and adjusted for the difference between observed and calculated values for the normal species.

TABLE 2: Rotational Constants for the Two Tunneling States of Conformer I of 1,3-Propanediol from the A-Reduction Hamiltonian

parameter	0^+ state	0^- state	theory	diff.
A (MHz)	7701.2351(18)[a]	7701.2376(17)[a]	7712.7	−0.15%
B (MHz)	3891.2952(14)	3891.2961(14)	3964.7	−1.9%
C (MHz)	2854.5575(12)	2854.5503(12)	2894.3	−1.4%
D_J (kHz)	2.362(34)	2.388(35)	2.24	−6.2%
D_{JK} (kHz)	0.18(20)	0.11(20)	1.03	
D_K (kHz)	2.24(44)	2.09(44)	0.921	−56%
δ_J (kHz)	0.754(11)	0.752(10)	0.709	−5.7%
δ_K (kHz)	3.88(54)	4.21(54)	4.04	−4.0%
ΔE (MHz)	5.4210(28)			
N_{lines}	158			
wt. std. dev.	0.97			

[a] Uncertainties shown in parentheses refer to the last digits shown and are type A, coverage factor $k = 2$ (two standard deviations).[19]

TABLE 3: Rotational Constants for the Two Tunneling States of Conformer II of 1,3-Propanediol from the A-Reduction Hamiltonian

parameter	0^+ State[a]	0^- State[a]	theory	diff.
A (MHz)	7586.7031(11)[b]	7586.7032(11)[b]	7581.4	0.1%
B (MHz)	3881.7118(5)	3881.7050(5)	3960.2	−2.0%
C (MHz)	2846.9390(5)	2846.9385(5)	2888.1	−1.4%
D_J (kHz)	2.512(17)	[c]	2.38	−5.2%
D_{JK} (kHz)	−1.510(56)	[c]	−1.05	−30%
D_K (kHz)	3.31(11)	[c]	2.62	−21%
δ_J (kHz)	0.8005(35)	[c]	0.756	−5.5%
δ_K (kHz)	3.858(37)	[c]	3.59	−6.9%
ΔE (MHz)	39.2265(24)			
N_{lines}	69			
rms (kHz)	4.3			
energy (kJmol^{-1})			1.28	

[a] The centrifugal distortion constants of the 0^+ and 0^- states were fitted to the same values. [b] Uncertainties shown in parentheses refer to the last digits shown and are type A, coverage factor $k = 2$ (two standard deviations).[19] [c] Parameters fixed at 0^+ state values.

The observed rotational constants agree to 1.6 MHz or better, which indicates that the structure calculations are quite satisfactory. Similarly, the fitted and calculated constants for the $^{13}C_4$ species are given in Table 5 and are also in good agreement. Finally, the tunneling splitting of 5.425 MHz is very similar to value of 5.421 MHz observed for the normal species as one might anticipate if the little C_4 motion occurs during the tunneling motion. The line assignments for the $^{13}C_3$ and the $^{13}C_5$ species are given in Table S7 of the Supporting Information and those for the $^{13}C_4$ species are given in Table S8 of the Supporting Information.

5. Dipole Moment Determination

One of the NIST FTMW spectrometers is equipped with set of 25 × 25 cm^2 parallel plates separated by 25 cm for Stark effect measurements. The plates are positioned along the cavity axis centered between the mirrors and the nozzle is located perpendicular to the cavity axis. Positive voltage is applied to one plate and an equal negative voltage is applied to the second plate to obtain Stark effect shifts in the transitions. The microwave electric field and external electric field are parallel so that $\Delta M = 0$ transitions are observed. The precise Stark plate separation was determined by a calibration with OCS $J = 1-0$ transition and the known dipole moment of $\mu = 2.3856(10) \times 10^{-30}$ C m [0.71519(3) D].[19,20]

For conformer I, the Stark shifted M = 0 components of the $1_{1,1} - 0_{0,0}$ b-type transition and $1_{1,0} - 0_{0,1}$ c-type transition were measured with applied voltages up to 2.5 kV (plus and minus 1.25 kV) with frequency shifts up to 1 MHz. The $M = 0$ and 1 components of the $2_{1,2} - 1_{0,1}$ b-type transition and $2_{1,1} - 1_{0,1}$ c-type transition were measured with voltages of up to 3 kV (plus and minus 1.5 kV) and a maximum shift of up to 1.1 MHz. In addition, the $M = 0$ and 1 components of the a-type $2_{0,2} - 1_{0,1}$, $2_{1,2} - 1_{1,1}$, and $2_{1,1} - 1_{1,0}$ transitions of the 0^+ and 0^- states were measured at voltages of up to 3 kV with shifts of up to 1.2 MHz. These Stark shifts were least-squares fit to the standard second-order asymmetric rotor coefficients of $(\mu_x E)^2$, where $x = a, b, c$, to derive the μ_a transition dipole moment between the 0^+ and 0^- states and the μ_b and μ_c dipole moment components listed in Table 6 with comparisons to the ab initio values, showing agreement to 0.15 D or better.

6. Astronomical Observations

Observations of 1,3-propanediol conformer I were made as part of the Green Bank Telescope (GBT) Prebiotic Interstellar Molecule Survey (PRIMOS) Legacy Project[21] between September 2007 and January 2009 with the NRAO 100 m Robert C. Byrd GBT. The GBT spectrometer was configured in its eight intermediate-frequency (IF), 200 or 800 MHz, three-level mode, which provides for observing four 200 MHz frequency bands or four 800 MHz frequency bands at a time in two polarizations through the use of offset oscillators in the IF part of the receiver. Antenna temperatures are on the T_A* scale[22] with estimated 20% uncertainties. The Sgr B2 (N-LMH) J2000 pointing position employed in azimuth and declination was $\alpha = 17^h47^m19.8^s$ and $\delta = -28°22'17''$, and a local standard of rest source velocity of +64 km s^{-1} was assumed. Data were taken in the OFF-ON position-switching mode, with the OFF position 60' east in azimuth with respect to the ON-source position. A single scan consisted of 2 min in the OFF-source position followed by 2 min in the ON-source position. Automatically updated dynamic pointing and focusing corrections were employed based on real-time temperature measurements of the structure input to a thermal model of the GBT; zero points were adjusted typically every 2 h or less using the quasar 1733−130 for calibration. The two polarization outputs from the spectrometer were averaged in the final data reduction process to improve the signal-to-noise ratio.

For 1,3-propanediol conformer I, 22 a-type transitions ($\mu_a = 2.9$ D, Table 6) were searched for as shown in Table 7. The full spectroscopic parameters of each transition including the calculated and measured rest frequencies, transition line strengths, and lower-level energies can be found in Table 7. No transitions were detected beyond the 1-sigma rms noise limit in any of the observed passbands. The lowest noise level attained was ∼5 mK near 47 900 MHz. Using the formalism presented by Hollis et al.[23] to calculate total column density and assuming a temperature of 10 K, which is consistent with other large organic species detected with the GBT toward the SgrB2N extended envelope,[23] we find an upper limit to the 1,3-propanediol conformer 1 total column density of $N_T < 2 \times 10^{13}$ cm^{-2}. This result is based on a rotational partition function of 36.5 T$^{1.5}$ derived from the measured A, B, and C rotational constants.

By way of comparison with the upper-limit column density for 1,3-propanediol, the measured abundance of glycolaldehyde ($CHOCH_2OH$) is $N_T \approx 3 \times 10^{14}$ cm^{-2} toward Sgr B2N,[24] and for ethylene glycol (CH_2OHCH_2OH) the measured abundance was found to be $N_T \approx 3.3 \times 10^{14}$ cm^{-2}.[4] Each of these species contain two carbon and oxygen atoms, whereas 1,3-propanediol

Downloaded by BOULDER LABORATORIES LBRY on September 3, 2015 | http://pubs.acs.org
Publication Date (Web): October 13, 2009 | doi: 10.1021/jp907564y

TABLE 4: Rotational Analysis of the ^{13}C Isotopologues of Conformer I of 1,3-Propanediol

parameter	$^{13}C_3$ obsd.	$^{13}C_3$ Calcd.	diff.	$^{13}C_5$ obsd.	$^{13}C_5$ Calcd.	diff.
A (MHz)	7670.9366(34)[a]	7670.55	0.39	7664.143(6)[a]	7663.33	0.81
B (MHz)	3839.3622(14)	3837.80	1.56	3844.500(3)	3843.17	1.33
C (MHz)	2823.4732(14)	2822.77	0.70	2827.169(3)	2826.55	0.62
D_J (kHz)	2.24(5)			2.49(12)		
D_{JK} (kHz)	1.23(15)			1.2(6)		
D_K (kHz)	1.5(8)			0 (fixed)		
δ_J (kHz)	0.696(14)			0.68(4)		
δ_K (kHz)	2.99(44)			3.6(6)		
N_{lines}	21			22		
rms (kHz)	2.5			8.5		

[a] Uncertainties shown in parentheses refer to the last digits shown and are type A, coverage factor $k = 2$ (two standard deviations).[19]

TABLE 5: Rotational Constants for the Two Tunneling States of $^{13}C_4$ Isotopologue of Conformer I of 1,3-Propanediol from the A-Reduction Hamiltonian

parameter	0^+ State[a]	0^+State[a]	theory	diff.
A (MHz)	7556.814(8)[b]	7556.778(6)[b]	7555.50	1.5
B (MHz)	3887.882(4)	3887.822(3)	3887.50	0.3
C (MHz)	2836.455(4)	2836.443(1)	2835.76	0.7
D_J (kHz)	2.12(13)			
D_{JK} (kHz)	0.0 (fixed)			
D_K (kHz)	3.2(13)			
δ_J (kHz)	0.86(11)			
δ_K (kHz)	3.5(6)			
ΔE (MHz)	5.425(8)			
N_{lines}	22			
rms (kHz)	10			

[a] The centrifugal distortion constants of the 0^+ and 0^- states were fitted to the same values. [b] Uncertainties shown in parentheses refer to the last digits shown and are type A, coverage factor $k = 2$ (two standard deviations).[19]

TABLE 6: Measured μ_a Transition Dipole Moment between the 0^+ and 0^- States and μ_b and μ_c Dipole Moments for 1,3-Propanediol Conformer I[a]

	exptl. 0^+ and 0^- states	MP2 conformer I
μ_a/D	2.917(1)[b,c]	3.01
μ_b/D	1.465(16)	1.62
μ_c/D	1.024(16)	1.16

[a] The calculated dipole moments at the MP2/aug-cc-pVTZ level are also given. [b] Uncertainties shown in parentheses refer to the last digits shown and are type A, coverage factor $k = 2$ (two standard deviations).[19] [c] For SI units, 1D (Debye) $= 3.336 \times 10^{-30}$ Cm.

has three carbon atoms. The upper-limit abundance for 1,3-propanediol is consistent with the assumption that, as molecular complexity increases, that is, adding a CH_2 group, the total column density of the molecule decreases. This is apparent given that the upper limit to the total column density of 1,3-propanediol is an order of magnitude lower than both $CHOCH_2OH$ and CH_2OHCH_2OH. A very similar result was reported recently for 1,2-propanediol,[4] adding to the growing body of evidence that saturated organic species with five or more heavy atoms that are at the limit of detection with current telescopes.

7. Discussion

In a recent FTMW study of 1,2-propanediol,[4] we reported the assignment of seven different conformers with zero-point-corrected (ZPE) energies up to 4.5 kJmol^{-1} (375 cm^{-1}). In the current study, only the two lowest-energy forms of 1,3-propanediol are observed. Whereas the next higher-energy conformer (V) lies at a relative ZPE energy of 3.5 kJmol^{-1} (287 cm^{-1}), as a result of its C_2 symmetry, only a small dipole moment remains along the b-axis (0.4 D). This substantially reduces the expected overall spectral intensity. All other conformers have energies above 5 kJmol^{-1} and therefore are expected to be below our detection limit[4] because of their small thermal population in the nozzle prior to expansion. From Figure 1, conformers I to IV all exhibit hydrogen bonds between the hydroxyl groups, whereas conformers V to VIII have no hydrogen bonding leading to elongated structures with small moments about the a-axis.

While not possible for 1,2-propanediol, tunneling splittings between equivalent structures are observed in both observed spectra of 1,3-propanediol. Furthermore, the observed transitions obey the same selection rules, that is, pure rotational transitions are b- and c-type, whereas a-type transitions cross between the inversion levels. Similar to inversion pathways discussed for one conformer of glycerol[25] (which has an additional OH group on the central carbon), these selection rules are expected for inversion between the two structurally chiral forms shown on the right and left sides of Figure 2. A remaining question of interest is, what is (are) the pathway(s) for the inversion?

Given the large 7-fold difference in tunneling frequencies, conformers I and II were initially anticipated to invert along independent tunneling pathways. The transition-state structures for pathways unique to each conformer were located using the Synchronous Transit-Guided Quasi-Newton approach[26] implemented in the *Gaussian 03* software package[6] and are shown as the central structures in the upper and lower parts of Figure 2. As found for glycerol, both transition states have C_S symmetry with one imaginary frequency and are located on pathways described by the counterclockwise and clockwise rotation of the two OH groups for I and II, respectively. The ZPE corrected barriers for these two routes are 1883 cm^{-1} and 1520 cm^{-1} for I and II, respectively. Therefore, in a qualitative sense, the 363 cm^{-1} decrease in the barrier for II relative to I may be argued to account for the 7-fold increase in the tunneling frequency of the former. It is further noted, however, that a comparable tunneling frequency of 41.9256(22) MHz was observed in glycerol[25] for a much lower transition-state barrier of 370 cm^{-1} (although for a more complex inversion route passing through a second set of minima at higher energy).

To obtain a more quantitative assessment of these possible tunneling pathways, a simple 1D WKB approach was used as described by Bicerano et al.[27,28] for the proton tunneling in malonaldehyde. This approximation is expected to be valid in the limit of small tunneling splittings as is certainly the case

Downloaded by BOULDER LABORATORIES LBRY on September 3, 2015 | http://pubs.acs.org
Publication Date (Web): October 13, 2009 | doi: 10.1021/jp907564y

TABLE 7: Transitions of 1,3-Propanediol Sought Toward in Sgr B2(N-LMH)

J'	K_a'	K_c'	v'	J''	K_a''	K_c''	v''	frequency/MHz	E/K	S_{ij}	T_A/mK
2	0	2	0	1	0	1	1	13301.949(2)[a]	0.324	1.979	<5
2	0	2	1	1	0	1	0	13301.949(2)	0.324	1.979	<5
2	1	1	0	1	1	0	1	14522.907(2)	0.557	1.500	<5
2	1	1	1	1	1	0	0	14533.744(2)	0.557	1.500	<5
4	0	4	0	3	0	3	1	25404.362(2)	1.901	3.863	<5
4	0	4	1	3	0	3	0	25415.065(2)	1.901	3.863	<5
5	0	5	0	4	0	4	1	31062.727(28)	3.119	4.818	<6
5	0	5	1	4	0	4	0	31073.351(31)	3.119	4.818	<6
6	1	6	0	5	1	5	1	36350.165(40)	4.641	5.773	<6
6	1	6	1	5	1	5	0	36360.665(44)	4.641	5.773	<6
6	0	6	0	5	0	5	1	36668.688(40)	4.611	5.796	<6
6	0	6	1	5	0	5	0	36679.197(43)	4.611	5.796	<6
6	1	5	0	5	1	4	1	41573.417(36)	5.361	5.639	<9
6	1	5	1	5	1	4	0	41584.094(34)	5.361	5.639	<9
7	1	7	0	6	1	6	1	42132.451(49)	6.386	6.778	<5
7	1	7	1	6	1	6	0	42142.817(54)	6.386	6.778	<5
7	0	7	0	6	0	6	1	42297.864(45)	6.371	6.787	<5
7	0	7	1	6	0	6	0	42308.237(54)	6.371	6.787	<5
8	1	8	0	7	1	7	1	47879.116(56)	8.408	7.779	<5
8	1	8	1	7	1	7	0	47889.326(64)	8.408	7.779	<5
8	0	8	0	7	0	7	1	47959.401(56)	8.401	7.783	<10
8	0	8	1	7	0	7	0	47969.615(63)	8.401	7.783	<10

[a] Uncertainties refer to the last digit and are type B coverage factor $k = 2$.[19]

Downloaded by BOULDER LABORATORIES LBRY on September 3, 2015 | http://pubs.acs.org
Publication Date (Web): October 13, 2009 | doi: 10.1021/jp907564y

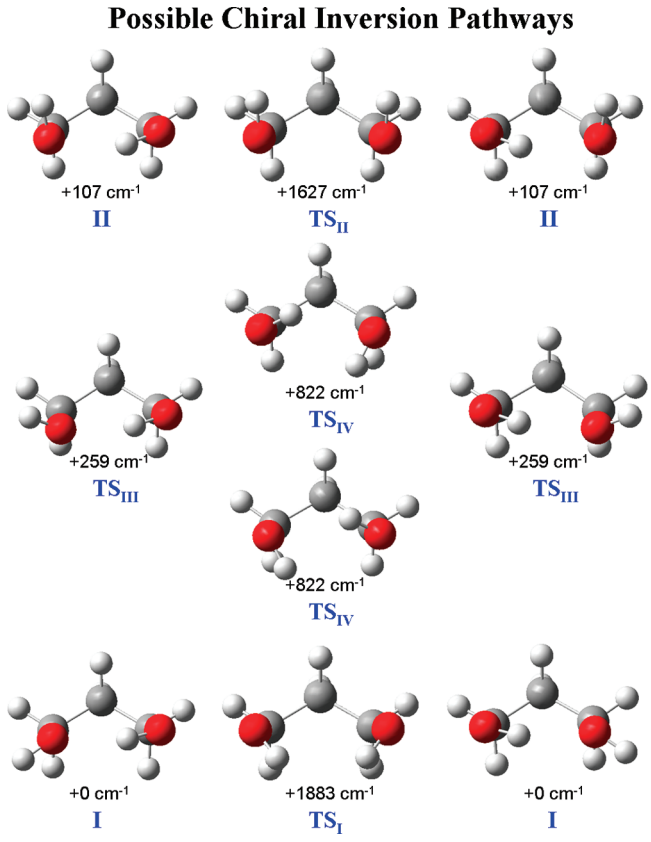

Figure 2. Three possible pathways for inversion that could explain the tunnelling split spectra of conformers I and II. The transition-state structures TS_{II} and TS_I for upper and lower pathways have C_S symmetry, whereas the TS_{IV} with C_1 symmetry exists as an enantiomeric pair. The transition-state structure is also illustrated for conformer interconversion (TS_{III}). The zero-point-corrected energies (MP2/aug-cc-pVTZ) are also given for each structure.

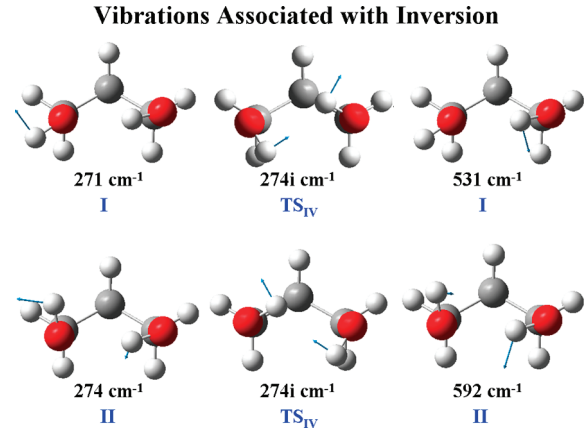

Figure 3. Normal mode (harmonic) displacements and frequencies associated with the concerted rotation of the two OH groups that define the inversion coordinate. The normal modes of the hydrogen bond accepting (free) OH group and the donating (bound) OH group and the mode with imaginary frequency of the TS_{IV} structure (and its mirror image) are shown.

for both conformer pairs observed here. The predicted level splitting, ΔE, from tunneling through a barrier approximated by an Eckart potential function may be obtained using the $F =$ $3n - 6$ ab initio vibrational frequencies ($\hbar\omega$) of I or II and of the transition-state structures, TS_I or TS_{II} ($\hbar\omega^*$), from

$$\Delta E = \frac{\hbar\omega_F}{\pi} e^{-\theta} \tag{1}$$

$$\theta = \frac{2\pi}{\hbar\omega_i}(V_{\text{eff}} - \sqrt{E_0 V_{\text{eff}}}) \tag{2}$$

$$V_{\text{eff}} = V_0 + \sum_{k=1}^{F-1} \frac{1}{2}(\hbar\omega_k^* - \hbar\omega_k) \tag{3}$$

where $E_0 = 0.5\,\hbar\omega_F$ and V_0 is the potential barrier without ZPE corrections, and $\hbar\omega_F$ and $\hbar\omega_i$ are the normal mode (torsional) frequencies of the equilibrium and transition-state structures respectively that are associated with the inversion coordinate.

TABLE 8: WKB Determinations of the Tunneling Splitting (MHz) for the Two Pairs of Inverting Structural Enantiomers Along 1D Torsional Pathways

		TS_I for I or TS_{II} for II [a]		TS_{IV} [a]	
conformer	ΔE	free OH	bound OH	free OH	bound OH
I	5.4210(28)[a]	7.3×10^{-6}	8.7×10^{-5}	2.96	17.0
II	39.2265(24)	2.2×10^{-19}	5.2×10^{-17}	21.9	136.7
II/I	7.236(4)	$<10^{-13}$	$<10^{-12}$	7.40	8.04
I ($^{13}C_4$)	5.425(8)	7.2×10^{-6}	8.7×10^{-5}	2.94	16.9

[a] TS_I, TS_{II}, and TS_{IV} are 2191 cm^{-1}, 1988 cm^{-1}, and 959 cm^{-1} (1883 cm^{-1}, 1627 cm^{-1} and 822 cm^{-1} with ZPE corrections) and have imaginary frequencies of 353 cm^{-1}, 142 cm^{-1}, and 274 cm^{-1}, respectively. [b] Uncertainties refer to the last digit and are type B coverage factor $k = 2$.[19]

The vector displacements and fundamental frequencies of the relevant normal modes for conformers I and II and those of the transition states are illustrated in Figure 3. The modes of the transition states ($\hbar\omega_i$) are simply those with the imaginary frequencies. As is evident from transition-state displacement vectors (and the equilibrium configurations), the inversion coordinate clearly involves the concerted rotation of the two OH groups, and therefore both the free (hydrogen bond acceptor) and bound (hydrogen bond donor) OH torsional modes need to be considered separately within this 1D model and are illustrated in Figure 3. For both conformers, the vibrational frequencies of the free OH are roughly half those of the bound OH.

The results of the WKB analysis are summarized in Table 8 for each of the OH torsional fundamentals ($\hbar\omega_F$). For either normal mode, the level splittings, ΔE, for conformer I inverting through TS_I and for II through TS_{II} are $<10^{-4}$ MHz and $<10^{-12}$ MHz, respectively. These tunneling splittings are orders-of-magnitude too small to account for observations. Further examination of the full 2D torsional surface for first-order saddle points revealed an enantiomeric pair of transition states of C_1 symmetry in the crossed dipole configurations (TS_{IV}) shown in the central part of Figure 2. The barrier heights of TS_{IV} are 959 cm^{-1} (822 cm^{-1} with ZPE corrections) relative to I and 876 cm^{-1} (715 cm^{-1}) relative to II. The predicted WKB level splittings given in Table 8 are 3.0 and 17 MHz for the free and bound OH fundamentals of conformer I and 22 and 140 MHz for conformer II, respectively. Therefore, for the inversion of both conformers through this common transition state, the limiting values from this 1D model nicely bracket the observed level splittings. Furthermore, the splitting ratios of II to I given in Table 8 are in excellent agreement with the observed ratio of 7.236. For conformer I, the very small change (<1%) in the level splitting with $^{13}C_4$ substitution is also reflected by the model predictions in Table 8, suggesting little impact of this atom on the tunneling dynamics. However, the other carbon atoms, $^{13}C_3$ and $^{13}C_5$, of the asymmetric structures play a larger role because the absence of level splittings in these cases indicate that the inversion tunneling is completely quenched.[28]

Closer examination of the coordinate displacements relative to the TS_{IV} structure in Figure 3 indicates that, for tunneling of the two conformers through mirror-image transition states, the magnitude of free OH rotation to reach TS_{IV} is larger than that of the bound OH. The relative importance of these displacements is also reflected in the similarity of free OH and TS_{IV} harmonic frequencies, suggesting the greater importance of this mode to the level splittings as the differences with the observed values would suggest. Given the simplicity of the WKB model compared to more rigorous treatments that might include a full reactive path formulation,[29] the agreement with the observed level splittings is quite good. Furthermore, the roughly 3-fold lower interconversion barrier from I to II (TS_{III} = 259 cm^{-1}) relative to that for inversion (TS_{IV} = 822 cm^{-1}) suggests that the wave functions of both conformers are partially delocalized over the four torsional surface minima. Therefore, a more rigorous treatment of the interconversion dynamics will require the full 2D torsional surface.

8. Conclusions

Tunneling splittings arising from chiral inversion of two conformers have been observed and fully assigned in the microwave spectrum of the sugar alcohol, 1,3-propanediol using cavity and broadband chirped-pulse FTMW techniques. The tunneling frequencies are found to increase by more than 7-fold from 5.4210(28) MHz to 39.2265(24) MHz for the two lowest-energy predicted conformers separated by 107 cm^{-1}. Three pathways for concerted OH torsional inversion have been theoretically investigated using a 1D WKB analysis and normal mode predictions at the MP2/aug-cc-pVTZ level of theory. Only the lowest-energy pathway having a common intermediate C_1 transition state for both conformers is identified as feasible from comparisons between the observed versus calculated splittings. Theoretical predictions of these and other transition states suggest the need to consider the full 2D OH torsional surface to arrive at a better understanding of the interconversion dynamics in this important sugar alcohol.

Acknowledgment. H. M. Pickett is gratefully acknowledged for providing the spectral fitting programs used in the analysis of the tunneling conformers. This work was supported by the NSF Centers for Chemical Innovation through grant 0847919.

Supporting Information Available: Theoretical structural parameters are available for all conformers at the MP2/aug-cc-pVTZ level. All observed and calculated transitions used in the fits are tabulated. This material is available free of charge via the Internet at http://pubs.acs.org.

References and Notes

(1) Hollis, J. M.; Lovas, F. J.; Jewell, P. R. *Astrophys. J.* **2000**, *540*, L107.

(2) Hollis, J. M.; Lovas, F. J.; Jewell, P. R.; Coudert, L. H. *Astrophys. J.* **2002**, *571*, L59.

(3) Cooper, G.; Kimmich, N.; Bellsle, W.; Sarinanna, J.; Brabham, K.; Garrel, L. *Nature* **2001**, *414*, 879.

(4) Lovas, F. J.; Plusquellic, D. F.; Pate, B. H.; Neill, J. L.; Muckle, M. T.; Remijan, A. J. *J. Mol. Spectrosc.* **2009**, *257*, 82.

(5) Caminati, W.; Melandri, S.; Favero, P. G. *J. Mol. Spectrosc.* **1995**, *171*, 394.

(6) Frisch, M. J.; Trucks, G. W.; Schlegel, H. B.; Scuseria, G. E.; Robb, M. A.; Cheeseman, J. R.; Montgomery, Jr., J. A.; Vreven T.; Kudin, K. N.; Burant, J. C.; Millam, J. M.; Iyengar, S. S.; Tomasi, J.; Barone, V.; Mennucci, B.; Cossi, M.; Scalmani, G.; Rega, N.; Petersson, G. A.; Nakatsuji, H.; Hada, M.; Ehara, M.; Toyota, K.; Fukuda, R.; Hasegawa, J.; Ishida, M.; Nakajima, T.; Honda, Y.; Kitao, O.; Nakai, H.; Klene, M.; Li, X.; Knox, J. E.; Hratchian, H. P.; Cross, J. B.; Adamo, C.; Jaramillo, J.; Gomperts, R.; Stratmann, R. E.; Yazyev, O.; Austin, A. J.; Cammi, R.; Pomelli; C.; Ochterski; J. W.; Ayala; P. Y.; Morokuma; K.; Voth; G. A.;

Downloaded by BOULDER LABORATORIES LBRY on September 3, 2015 | http://pubs.acs.org
Publication Date (Web): October 13, 2009 | doi: 10.1021/jp907564y

Salvador; P.; Dannenberg; J. J.; Zakrzewski; V. G.; Dapprich; S.; Daniels; A. D.; Strain; M. C.; Farkas; O.; Malick; D. K.; D. Rabuck; A.; Raghavachari; K.; Foresman; J. B.; Ortiz; J. V.; Cui; Q.; Baboul; A. G.; Clifford; S.; Cioslowski; J.; Stefanov; B. B.; Liu; G.; Liashenko; A.; Piskorz; P.; Komaromi; I.; Martin; R. L.; Fox; D. J.; Keith; T.; Al-Laham; M. A.; Peng; C. Y.; Nanayakkara; A.; Challacombe; M.; Gill; P. M.W.; Johnson; B.; Chen; W.; Wong; M. W.; Gonzalez; C.; Pople; J. A. *Gaussian 03*, Rev. B.04; Gaussian Inc.: Pittsburgh, PA; 2003.

(7) Møller, C.; Plesset, M. S. *Phys. Rev.* **1934**, *46*, 618. Head-Gordon, M.; Pople, J. A.; Frisch, M. J. *Chem. Phys. Lett.* **1988**, *153*, 503.

(8) Dunning, T. H., Jr. *J. Chem. Phys.* **1989**, *90*, 1007. Woon, D. E.; Dunning, T. H., Jr. *J. Chem. Phys.* **1993**, *98*, 1358.

(9) Vázquez, S.; Mosquera, R. A.; Rios, M. A.; van Alsenoy, C. *J. Mol. Struct. (Theochem)* **1988**, *181*, 149.

(10) Rubinson, K. A; Hubbard, J. *Polymer* **2009**, *50*, 2618.

(11) Balle, T. J.; Flygare, W. *Rev. Sci. Instrum.* **1981**, *52*, 33.

(12) Lovas, F. J.; Suenram, R. D. *J. Chem. Phys.* **1987**, *87*, 2010.

(13) Suenram, R. D.; Grabow, J.-U.; Zuban, A.; Leonov, I. *Rev. Sci. Instrum.* **1999**, *70*, 2127.

(14) Grabow, J.-U.; Stahl, W. *Z. Naturforsch., A* **1990**, *45*, 1043. Grabow, J.-U.; Stahl, W.; Dreizler, H. *Rev. Sci. Instrum.* **1996**, *67*, 4072.

(15) Grabow, J.-U. private communication 2003; see www.pci.uni-hannover.de/~lgpca/spectroscopy/ftmw/.

(16) Brown, G. G.; Dian, B. C.; Douglass, K. O.; Geyer, S. M.; Shipman, S. T.; Pate, B. H. *Rev. Sci. Instrum.* **2008**, *79*, 53103–1.

(17) Certain commercial products are identified in this article to specify adequately the experimental or theoretical procedures. In no case does such identification imply recommendation or endorsement by the National Institute of Standards and Technology nor does it imply that the products are necessarily the best available for the purpose.

(18) Pickett, H. M. *J. Mol. Spectrosc.* **1991**, *148*, 371. The SPFIT/SPCAT package is available at http://spec.jpl.nasa.gov.

(19) Taylor, B. N.; Kuyatt, C. E. *NIST Tech. Note* **1994**, *1297*, 1. The publication may be downloaded from http://physics.nist.gov/Pubs/guidelines/contents.html.

(20) Reinartz, J. M. L. J.; Dymanus, A. *Chem. Phys. Lett.* **1974**, *24*, 346.

(21) See http://www.cv.nrao.edu/~aremijan/PRIMOS/ for more information on the project.

(22) Ulich, B. L.; Haas, R. W. *Astrophys. J. Suppl.* **1976**, *30*, 247.

(23) Hollis, J. M.; Jewell, P, R.; Lovas, F. J.; Remijan, A. *Astrophys. J.* **2004**, *613*, L45.

(24) Hollis, J. M. *Proc. IAU Symp. No.* **2006**, *231*, 227.

(25) Ilyushin, V. V.; Motiyenko, R. A.; Lovas, F. J.; Plusquellic, D. F. *J. Mol. Spectrosc.* **2008**, *251*, 129.

(26) Peng, C.; Ayala, P. Y.; Schlegel, H. B.; Frisch, M. J. *J. Comput. Chem.* **1996**, *17*, 49. Peng, C.; Schlegel, H. B. *Israel J. Chem.* **1993**, *33*, 449.

(27) Bicerano, J.; Schaefer III, H. F.; Miller, W. H. *J. Am. Chem. Soc.* **1983**, *105*, 2550.

(28) Keske, J. C.; Blake, T. A.; Lin, W.; Pringle, W. C.; Novick, S. E.; Plusquellic, D. F. *J. Chem. Phys.* **2006**, *124*, 074309.

(29) Carrington, T.; Miller, W. H. *J. Chem. Phys.* **1986**, *84*, 4364. Ruf, B. A.; Miller, W. H. *J. Am. Chem. Soc. Faraday Trans. II* **1988**, *84*, 1523.

JP907564Y

Downloaded by BOULDER LABORATORIES LBRY on September 3, 2015 | http://pubs.acs.org
Publication Date (Web): October 13, 2009 | doi: 10.1021/jp907564y